Intereference effects on Z-shaped Model Support Sting Data in T-38 Wind Tunnel

Dijana Damljanović, BSc (Eng)[1)]
Aleksandar Vitić, BSc (Eng)[1)]

In this paper a brief discussion of the forms of interference occurring in subsonic and transonic test section of the wind tunnel *T-38* due to the model support system is given. Two types of model attachments, rear normal sting and *Z-shaped sting*, are considered. Shapes and magnitude of interference are given for particular examples. Except at the axial force coefficient C_A, the main interference is at the pitching moment coefficient C_m. A procedure for eliminating the undesired effect is given in this paper

Key words: **wind tunnel, aerodynamic testing, aerodynamic model, aerodynamic coefficient, subsonic flow, transonic flow.**

Used symbols

M	– Mach number in the test section of T-38 wind tunnel
$P_0\,[\text{bar}]$	– Stagnation pressure in the test section of the T-38 wind tunnel
$Pst\,[\text{bar}]$	– Static pressure in the test section of the T-38 wind tunnel
$Pb\,[\text{bar}]$	– Base pressure
$q\,[\text{bar}]$	– Dynamic pressure in the test section of the T-38 wind tunnel
$M\,Re\,[\text{l/m}]$	– Reynolds number in the test section of the T-38 wind tunnel
$T_0\,[\text{K}]$	– Stagnation temperature in test section of T-38 wind tunnel
$D\,[\text{m}]$	– Referent diameter of the model
$L\,[\text{m}]$	– Length of the model
$d\,[\text{m}]$	– Diameter of the model support sting
$l\,[\text{m}]$	– Effective sting length
$(d/D)_{cr}$	– Critical sting diameter
$(l/D)_{cr}$	– Critical sting length
$\alpha',\ alfa'\ [^{\circ}]$	– Total angle of model attack
$\beta'\ [^{\circ}]$	– Total angle of model sideslip
$\phi'\ [^{\circ}]$	– Total angle of model roll
$\phi a'\ [^{\circ}]$	– Roll angle of the flow plane
C_N	– Normal force coefficient
C_m	– Pitching moment coefficient
C_A	– Axial force coefficient
C_{N_0}	– Normal force coefficient for $\alpha' = 0^{\circ}$
C_{m_0}	– Pitching moment coefficient for $\alpha' = 0^{\circ}$
C_{A_0}	– Axial force coefficient for $\alpha' = 0^{\circ}$
ΔC_{N_0}	– Difference of the normal force coefficients of the model mounted on Z-shaped and rear normal stings
ΔC_{m_0}	– Difference of the pitching moment coefficients of the model mounted on the Z-shaped and rear normal stings
ΔC_{A_0}	– Difference of the axial force coefficients of the model mounted on the Z-shaped and rear normal stings
$C_{x\ measured}$	– Drag force coefficient of the model mounted on support sting
C_x	– Drag force coefficient of the model without support sting
$C_{x\ normal\ sting}$	– Contribution at drag force coefficient consequence of a rear normal sting
$C_{xZ\ sting}$	– Contribution at drag force coefficient consequence of a Z-shaped sting
RSN	– Run Sequence Number
$3DTR$	– Transonic test section identification
$3DPO$	– Subsonic test section identification
$Configuration$	– Model configuration identifier
$dV,\ [^{\circ}]$	– Total angle of fin altitude
$dP,\ [^{\circ}]$	– Total angle of fin straight
$dR,\ [^{\circ}]$	– Total angle of fin rotation
Xp	– Axis identification (unrotated body axes system)
Yp	– Axis identification (unrotated body axes system)
Zp	– Axis identification (unrotated body axes system)
$Body$	– Body of the model missile identifier
$Wing$	– Wing of the model missile identifier
Fin	– Fin of the model missile identifier

[1)] Military Technical Institute (VTI), Ratka Resanovića 1, 11132 Belgrade, SERBIA

Introduction

NOWADAYS very different model support stings are being used, from simple rear normal sting to the bent sting with the angle from 90 degrees relation to the direction of the airflow. Z-shaped stings are also used, primarily depending on the model geometry and test program requirements. Experimental aerodynamics has been dealing with many questions concerning model support sting interference effects on the data obtained in trisonic wind tunnels [1-3]. Base pressure and base drag are significantly affected by the support interference, but also body drag, lift, static moment and damping derivatives. The effect of typical sting diameters on the base pressure is shown in Fig.1
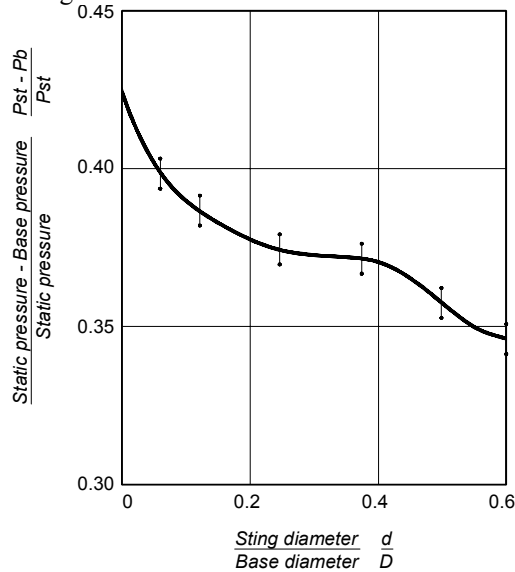
Figure 1. The effect of the sting diameter to model base diameter ratio on the ratio of difference of static and base pressure to the static pressure for an ogive cylinder model; M = 2.97 and MRe = 15, [1]

The effect of Reynolds number on the critical sting length is shown in Fig.2.
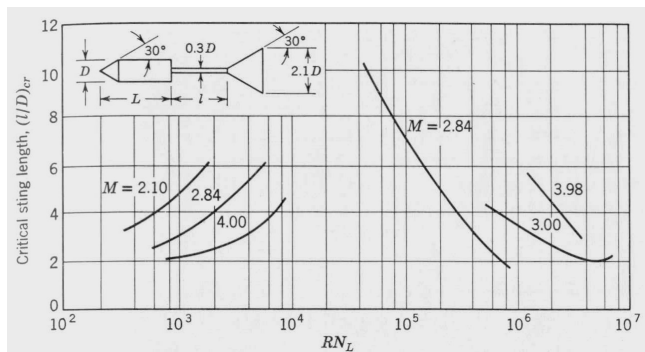

Figure 2. The effect of Reynolds number on the critical sting length, [1]

Critical sting length, $(l/D)_{cr}$ is defined as the shortest sting length, which does not change the constant base pressure level, obtained by longer stings. Effective sting length, l is defined as distance from the model base to the first large increase of sting diameter (generally a conic taper to a large diameter). Critical sting diameter, $(d/D)_{cr}$ is defined as the largest sting diameter, which does not change the constant base pressure level, obtained by smaller diameter stings. Figures 3 and 4 show *AGARD B* and *AGARD C* calibration models with lengths and diameters of the model support stings, the effects of which are insignificant for the wind tunnels data.
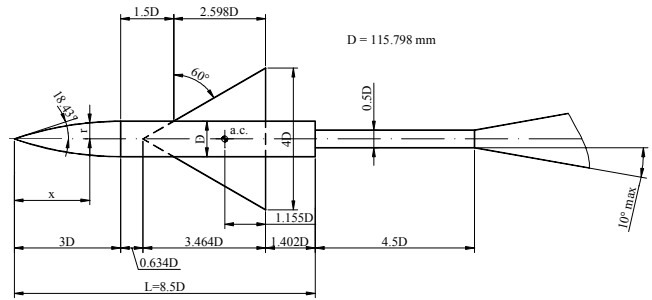

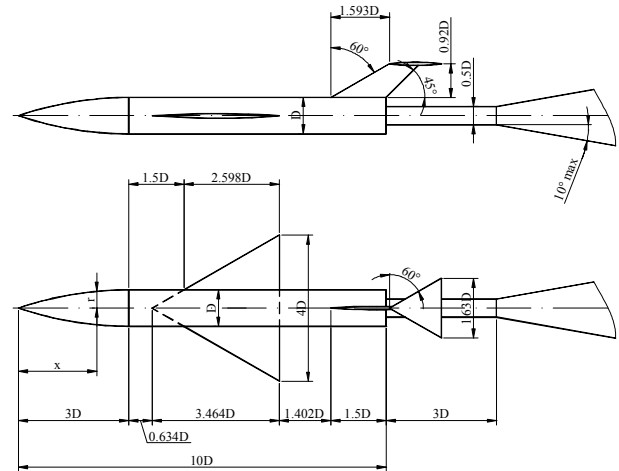**Figure 3.** *AGARD B* model

Figure 4. *AGARD C* model

The P22 model is chosen for the experiment. The test program has been conducted for the purpose of evaluating Z-shaped model support sting effects on the measurements data. The majority of this program has used aerodynamics forces and moments as interference indicators. The model base pressure was not measured because of fuselage rear part shape. The experiment was initiated for the purpose of improving the understanding of some problems associated with Z-shaped model support sting at subsonic and transonic Mach numbers in the T-38 wind tunnel.

Wind Tunnel T-38

T38 wind tunnel in VTI is a blowdown-type pressurized wind tunnel with 1.5 x 1.5 m square test section. Fig.5 shows P22 model in the test section of the T38 wind tunnel. The test section for subsonic and supersonic tests has solid walls and for transonic tests a section with porosity walls is inserted in to the tunnel configuration. The porosity of walls can be varied between 1.5% and 8% depending on the Mach number to achieve the best flow quality.

Figure 5. P22 model in the test section of the T38 wind tunnel

Mach numbers in the range 0.2 to 4.0 can be achieved in the test section with Reynolds numbers up to 115 million per meter. Sidewall flaps in the tunnel diffuser set Mach number in the subsonic configuration. In the supersonic configuration Mach number is set by the flexible nozzle contour, while in the transonic configuration Mach number is set both by the sidewall flaps and the flexible nozzle and actively regulated by blow-off system. Mach number can be set and regulated to within 0.3% of the nominal value.

Stagnation pressure in the test section can be maintained between 1.1 and 15 bar depending on the Mach number and of regulated to 0.3% of the nominal value. Run times are in the range the 6 s to 60 s depending on the Mach number and stagnation pressure.

Model in the test section is supported by the rear normal or Z-shaped sting mounted on a pitch-and-roll mechanism. It is possible to achieve the desired aerodynamic angles by this mechanism, in the pitch angle range $-12°$ to $+21°$ and in the roll angle range $0°$ to $360°$. The facility supports both continuous and step-by-step model movements during measurement. Position accuracy is $\pm0.05°$ in the pitch and $\pm0.25°$ in the roll.

Instrumentation, data recording and data reduction

The stagnation pressure P_0 in the test section was measured by *Mensor* quartz bourdon tube absolute pressure transducers pneumatically connected to a pitot probe in the settling chamber of the wind tunnel. Range of the used transducers is 7 bar. The nonlinearity and hysteresis of this transducer is typically 0.02 % F.S. A calibration of the transducer was performed using a *Mensor* quartz secondary pressure standard.

The difference $Pst - P_0$ between the stagnation and static pressure in the subsonic test section was measured by a *Mensor* quartz bourdon tube differential pressure transducer pneumatically connected to the pitot probe and to an orifice on the test section sidewall. The range of this transducer is 1.75 bar. The nonlinearity and hysteresis of this transducer is also 0.02 % F.S. This transducer was calibrated in the same manner as the P_0 transducer.

The static pressure Pst in the transonic test section was measured by a *Mensor* quartz bourdon tube absolute pressure transducer pneumatically connected to an orifice on the sidewall of the test section. The range of this transducer is 1.75 bar. The nonlinearity and hysteresis of this transducer is also 0.02 % F.S. This transducer was calibrated in the same manner as the P_0 transducer.

The stagnation temperature T_0 was measured by a *RTD* probe in the settling chamber of the wind tunnel. The accuracy of this transducer is approximately ±0.5 K.

Resolvers mounted on the mechanism measured the pitching and rolling angles of the model support. The resolution of the pitching angle resolver is $\pm0.05°$ and of the rolling angle resolver is $\pm0.25°$.

The *VTI40A* internal six-component strain gage balance measured aerodynamic forces and moments acting on the model. The accuracy of the used balance is approximately 0.3% F.S. The balance was calibrated prior to testing [4]. In these wind tunnel tests the balance was mounted on Z-shaped sting and rear normal sting.

The output of a precision digital clock was sampled synchronously with other channels in order to serve as time base for the segmentation of data.

The data acquisition system consisted of *Teledyne* 64 channels "front-end" controlled by *PC Compaq* computer. The front-end channels for flow parameters transducers were set with 10 Hz, fourth-order low pass Butterworth filters and appropriate amplification.

In order to minimize the differences in time lags on various channels during model sweep, the channels for six balance components were set with 30 Hz low pass filters of the same type. In order to compensate for the poorer filtering on these channels these signals were additionally filtered during the data reduction by a 3 Hz non-causal low pass digital filter.

The data from all analog channels were digitized by a 16-bit resolution *A/D* converter with overall accuracy of the acquisition system being about 0.1% F.S. of the channels signal range. All channels were sampled with the same 200 samples/s rate.

Digitized data were received on a *Compaq AlphaServer DS20E* computer and stored on a disk for later reduction.

Data reduction was performed after each run, using the standard T38 *Application Software package* in use with wind tunnel facility. It was done in several stages, i.e.:
- Data acquisition system interfacing and signal normalization;
- Determination of flow parameters;
- Determination of model attitude;
- Determination of aerodynamic coefficients.

A different software module was performing each stage.

The axes system used for presenting the results in this report is the unrotated body axes system, (see Fig.6). The origin of this axes system is in the model reference point. The Xp axis is parallel to the longitudinal axis and positive towards the tail of the model. The Zp axis lies in a plane whose orientation is chosen as parallel to the "nominal" orientation of the flow plane (i.e. in the pitch plane model support mechanism) and it is positive in the same direction as the cross-flow component of the air velocity relative to the model when α' is positive. The Yp axis completes the right-hand coordinate system. The angle of attack α' is the angle between the projection of the air velocity vector on the $XpZp$ plane and model axis. The angle β' is the angle between the air velocity vector and the $XpZp$ plane. The roll angle ϕ' is the angle between the model plane of the left-right symmetry and the $XpZp$ plane. The third aerodynamic angle ϕ'_a describes the position of the $XpZp$ plane relative to the wind tunnel vertical plane of the symmetry, when both α' and β' are equal to zero.
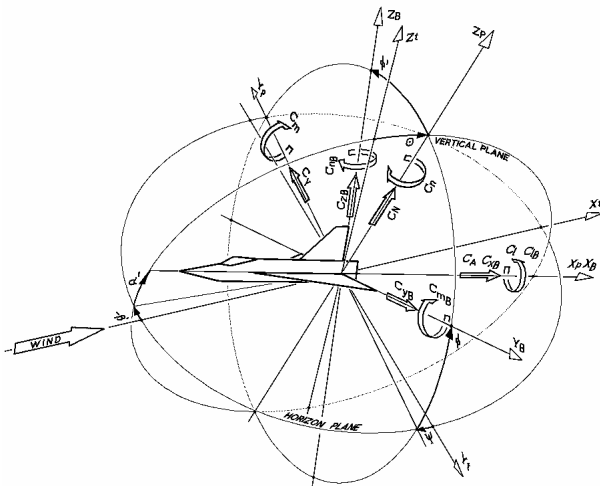
Figure 6. Axes system used in data reduction

Model

The P22 model has a cylindrical body with wings, horizontal and vertical tail. The length of the model was chosen with respect to the tunnel test section size, determining the scaling of the other dimensions. Basic model dimensions are given in Figures 7 and 8.

For these tests, a multi-piece steel-and-aluminum model was made. It was designed, manufactured, checked and assembled in the workshop of the Military Technical Institute. Checking of the model dimensions showed that it was in accordance with the requirements.

Model support stings

Most model support stings used in the T-38 wind tunnel have been manufactured in the workshop of the Military Technical Institute. There are a wide variety of differently shaped stings available: straight, bent, *Z*-shaped and other special stings.

In the first part of the testing, the P22 model was mounted on a *Z*-shaped sting shown in Fig.7. The diameter of the straight part of the *Z*-shaped sting is 50 mm. To see what effects of the used *Z*-shaped sting on aerodynamic results are, in the second part of the testing, P22 model was mounted on a rear normal sting shown in Fig.8.
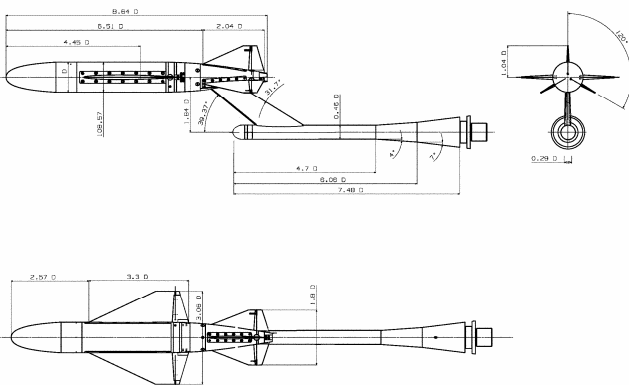
Figure 7. P22 model mounted on *Z*-shaped sting
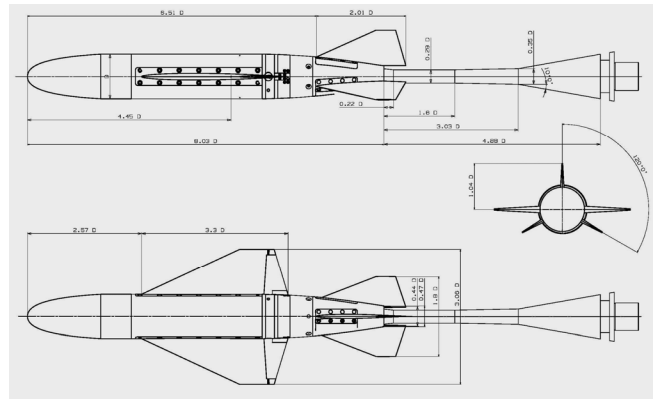
Figure 8. *P22* model mounted on rear normal sting

Test program with *Z*-shaped and rear normal stings

A general summary of the test program for the P22 model mounted on a *Z*-shaped sting is given in Table 1.

Table 1.

RSN	Configuration	M	MRe, 1/m	P_0 bar	$\phi°$	$dV°$	$dP°$	$dR°$
49	Body	0.95	3.56	2.30	0	-	-	-
10	BodyWingFin	0.3	1.78	2.50	0	0	0	0
86	BodyWingFin	0.7	3.06	2.30	0	0	0	0
4	BodyWingFin	0.95	3.55	2.30	0	0	0	0

A general summary of the test program for the P22 model mounted on a rear normal sting is given in Table 2.

Table 2.

RSN	Configuration	M	MRe, 1/m	P_0 bar	$\phi°$	$dV°$	$dP°$	$dR°$
125	Body	0.95	3.50	2.30	0	-	-	-
130	BodyWingFin	0.3	1.64	2.50	0	0	0	0
129	BodyWingFin	0.7	3.03	2.30	0	0	0	0
126	BodyWingFin	0.95	3.50	2.30	0	0	0	0

Test results are available at Mach number M = 0.95 for *Body* model configuration for both *Z*-shaped sting and rear normal sting.

Test results are available at Mach numbers M = 0.3, M = 0.7 and M = 0.95 for *BodyWingFin* model configuration for both Z-shaped sting and rear normal sting.

Results and Discussion

Figures 9 - 11 show the aerodynamic coefficients C_N, C_m and C_A for *Body* model configuration mounted on the *Z* -shaped and rear normal stings.

Figures 12 - 20 show the aerodynamic coefficients C_N, C_m and C_A for *BodyWingFin* model configuration mounted on the *Z*-shaped and rear normal stings.
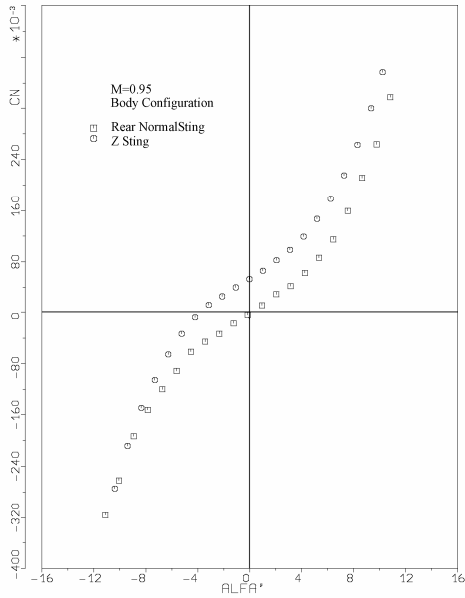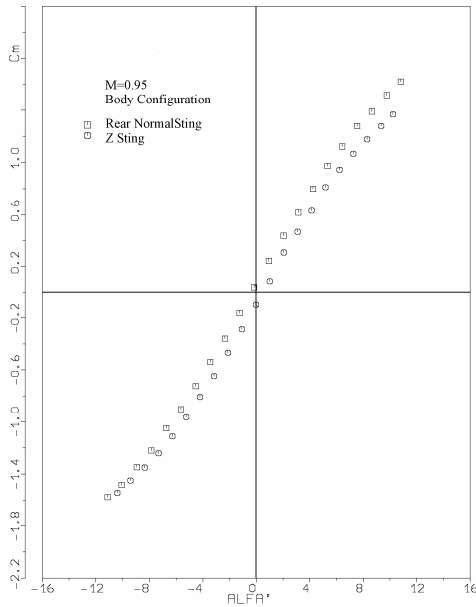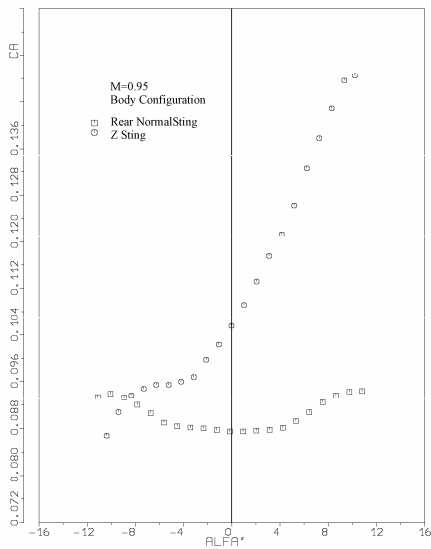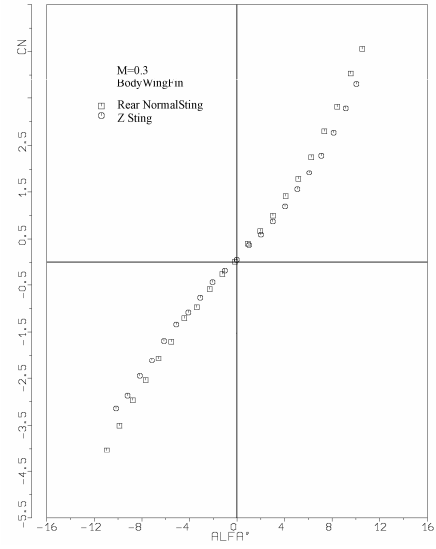
Figure 9.

Figure 12
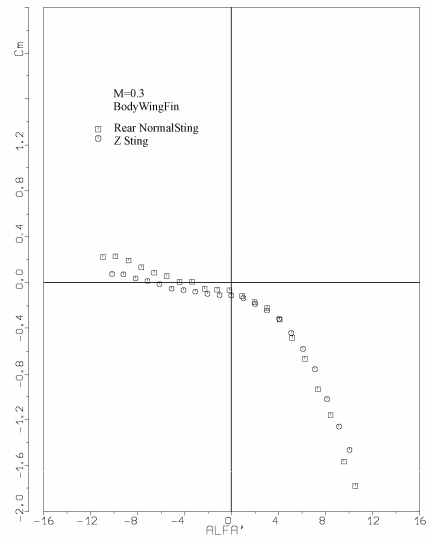
Figure 10
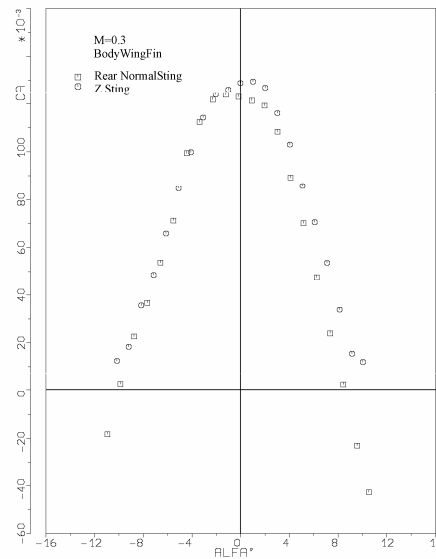
Figure 13
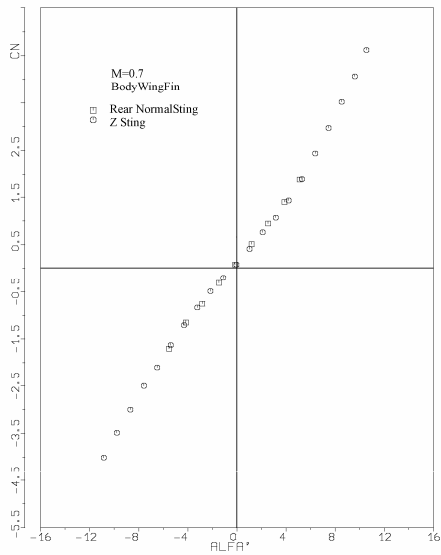
Figure 11

Figure 14

Figure 15
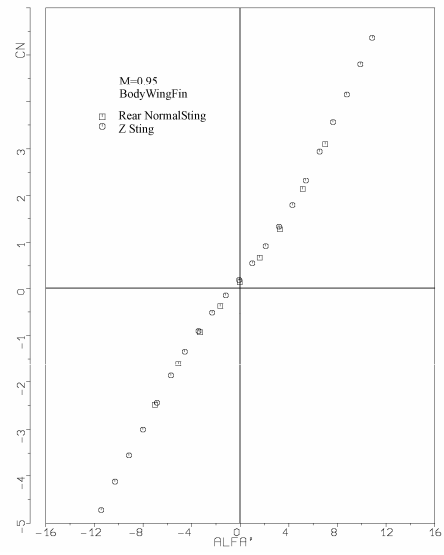
Figure 18
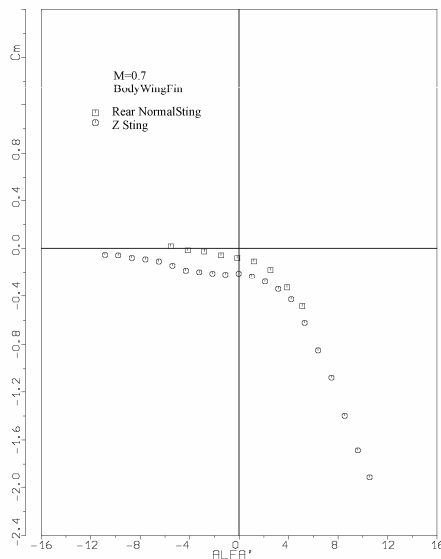
Figure 16

Figure 19

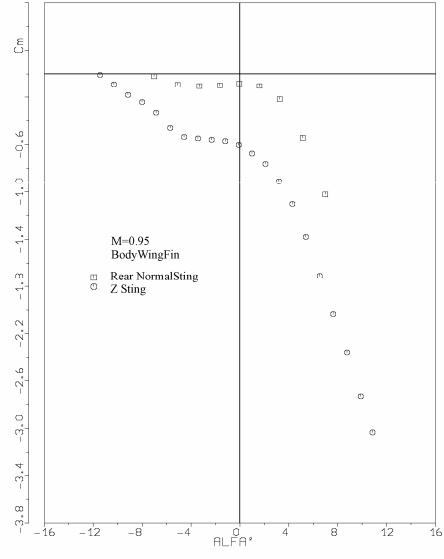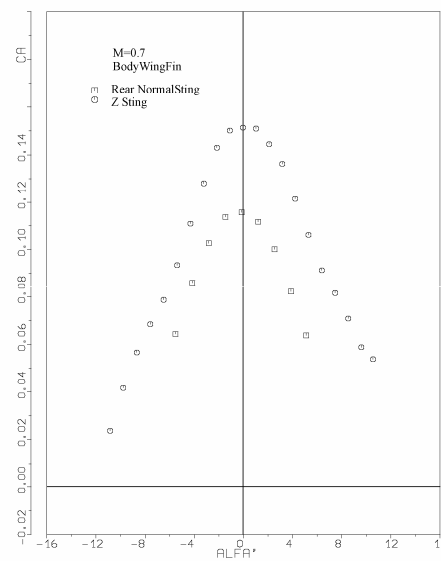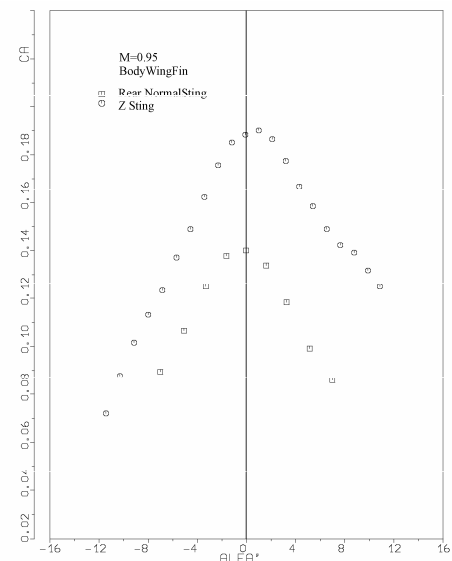**Figure 17**

Figure 20

A general summary of the interference effects for this particular model configuration is given in Tables 3 - 6.

Table 3. Interference effects of the sting type on aerodynamic coefficients for M = 0.95

MODEL CONFIGURATION	RSN	C_{N0}	C_{m0}	C_{A0}	REMARKS
BODY ON Z-SHAPED STING	49	0.053	-0.092	0.1055	ALFA'=0
BODY ON REAR NORMAL STING	125	-0.004	0.040	0.0875	ALFA'=0
$\Delta C_{N0}, \Delta C_{m0}, \Delta C_{A0}$		0.057	-0.132	0.018	ALFA'=0

Table 4. Interference effects of the sting type on aerodynamic coefficients for M = 0.30

MODEL CONFIGURATION	RSN	C_{N0}	C_{m0}	C_{A0}	REMARKS
BODYWINGFIN ON Z-SHAPED STING	10	0.058	-0.110	0.1288	ALFA'=0
BODYWINGFIN ON REAR NORMAL STING	130	0.014	-0.065	0.1229	ALFA'=0
$\Delta C_{N0}, \Delta C_{m0}, \Delta C_{A0}$		0.044	-0.045	0.006	ALFA'=0

Table 5. Interference effects of the sting type on aerodynamic coefficients for M = 0.70

MODEL CONFIGURATION	RSN	C_{N0}	C_{m0}	C_{A0}	REMARKS
BODYWINGFIN ON Z-SHAPED STING	86	0.080	-0.209	0.1514	ALFA'=0
BODYWINGFIN ON REAR NORMAL STING	129	0.081	-0.079	0.1157	ALFA'=0
$\Delta C_{N0}, \Delta C_{m0}, \Delta C_{A0}$		-0.001	-0.130	0.0357	ALFA'=0

Table 6. Interference effects of the sting type on aerodynamic coefficients for M = 0.95

MODEL CONFIGURATION	RSN	C_{N0}	C_{m0}	C_{A0}	REMARKS
BODYWINGFIN ON Z-SHAPED STING	4	0.178	-0.603	0.1883	ALFA'=0
BODYWINGFIN ON REAR NORMAL STING	126	0.132	-0.081	0.1401	ALFA'=0
$\Delta C_{N0}, \Delta C_{m0}, \Delta C_{A0}$		0.046	-0.522	0.0482	ALFA'=0

In Figures 21 - 23 these effects are shown in the form of graphs. The difference of coefficients ΔC_{N0}, ΔC_{m0} and ΔC_{A0} from wind tunnel testing of the *P22* model on Z-shaped and rear normal stings is given as function of Mach number. The biggest interference effects of the sting type on the test results as function of Mach number are noticeable in that way. Symbol *"0"* means that the aerodynamic coefficients are for the model angle of attack $\alpha' = 0°$. From these graphs it can be concluded that the interference effects of the *Z*-shaped sting are the smallest at normal force coefficient C_{N0} and significant at pitching moment coefficient C_{m0} and axial force coefficient C_{A0}.

It should be noted that the analysis did not determine the absolute interference of the *Z*-shaped sting on the test results of aerodynamic measurement on *P22* model, but relative, as difference of *Z*-shaped and rear normal stings interference. Furthermore, the test results are valid only for *P22* model and they will take different values for other models of testing. The obtained test results can not be generalized. Experiment has shown that there are significant differences in the obtained test results using *Z*-shaped sting and rear normal sting, which was confirmed during *P22* model wind tunnel testing.

It was seen that it is not possible to physically eliminate the sting interference effects on the model data. However, there is a possibility for eliminating the sting interference effects, for e.g. through these three steps.
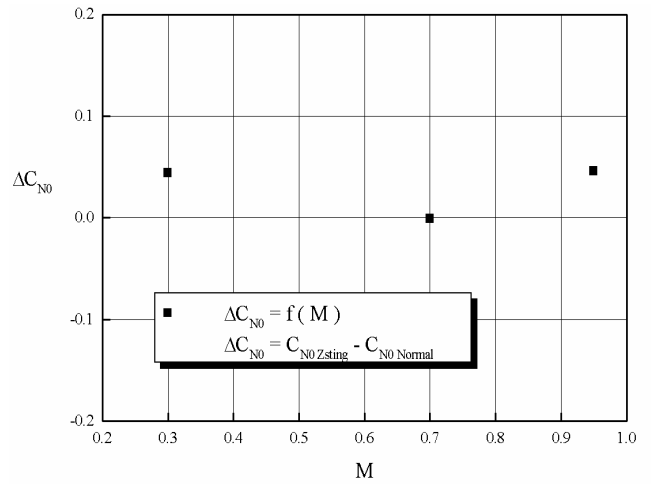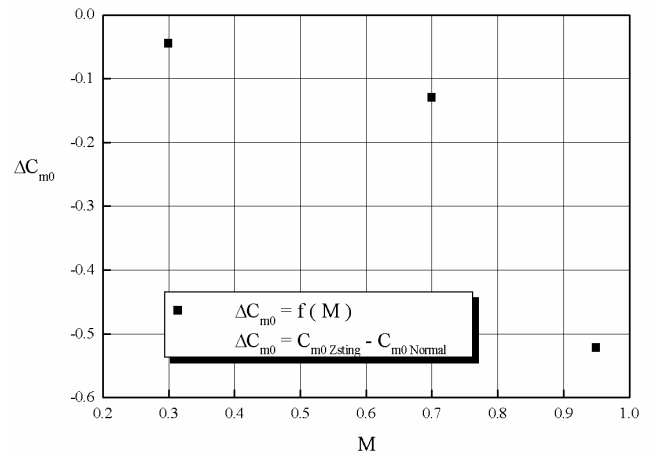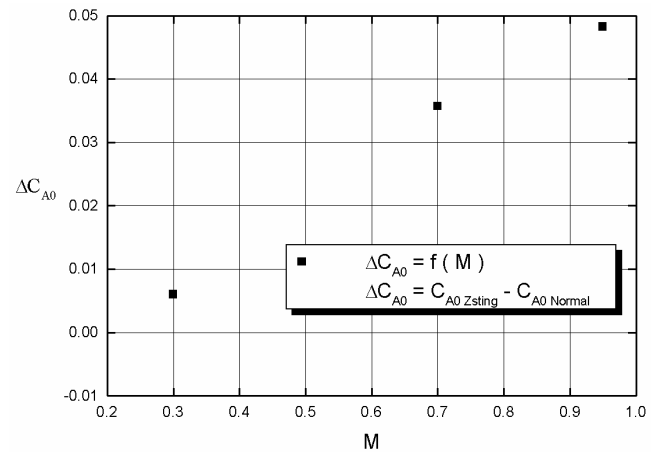

Figure 21.

Figure 22.

Figure 23.

In the first step, (see Fig.24) the model mounting-sting is a rear normal sting. Drag force coefficient for the model is:

$$C_{x\,measured} = C_x + C_{x\,normal\,sting} \qquad (A)$$

$C_{x\,normal\,sting}$ is the contribution at drag force coefficient consequence of the rear normal sting.
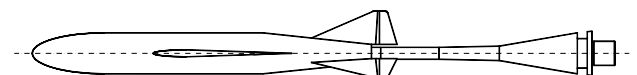

Figure 24.

In the second step, (see Fig.25), the model mounting-sting is the Z-shaped sting and rear normal sting is leaned against the model. Drag force coefficient for the model is:

$$C_{x\,\text{measured}} = C_x + C_{x\,Z\,\text{sting}} + C_{x\,\text{normal sting}} \qquad (B)$$

$C_{x\,Z\,\text{sting}}$ is the contribution at drag force coefficient consequence of the Z-shaped sting.
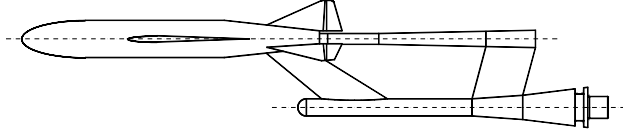

Figure 25.

And, finally, in the third step, (see Fig.26), the model mounting-sting is the Z-shaped sting. Drag force coefficient for the model is:

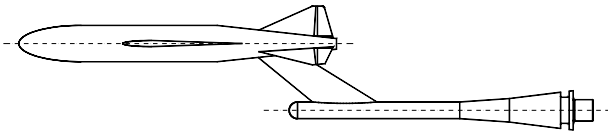$$C_{x\,\text{measured}} = C_x + C_{x\,Z\,\text{sting}} \qquad (C)$$

Figure 26.

If equation C is subtracted from equation B, the contribution at drag force coefficient consequence of a rear normal sting is obtained.

$$B - C = C_{x\,\text{normal sting}} \qquad (D)$$

If equation D is subtracted from equation A, the "true" drag force coefficient is obtained.

$$A - D = C_x \qquad (E)$$

It is shown that it is possible to eliminate the sting interference effects on the model data through serial measurements.

Conclusions

Some collected results from the wind tunnel tests with *P22* model confirm the existence of significant interference terms from the Z-shaped sting on the model. It is shown that Z-shaped sting will create a gradient of pressure on the rear body giving rise to an axial buoyancy force. Z-shaped sting produces the change of pressure on the lower surface of the horizontal tail with changing of the aerodynamic force on the tail and pitching moment. Interference effects from the Z-shaped sting are rising with Mach number increasing.

The interference cannot be physically eliminated and its effects will have to be allowed for in the planning of test experiments in the wind tunnel *T38*. Interference of the Z-shaped sting on the results of the measurement could be reduced to the minimum level if the tested model is without rear tails. The other possibility is to use the suggested procedure.

References

[1] ALAN POPE, KENNITH GOIN, *High-speed Wind Tunnel testing*, John Wiley and sons, Inc London.

[2] CARTER,E.C.: *Interference effects of model support systems*, Aircraft Research Association Limited Manton Lane, Bedford, UK

[3] TUNNEL,P.J.: *An investigation of sting support interference on base pressure and fore body chord force at Mach numbers from 0 to 1.3*, NACA RM A54K16A

[4] JANJIKOPANJI,G.: *Baždarenje aerovage VTI40A*, Vojnotehnički institut, Beograd.

Uticaj *Z* držača modela na rezultate merenja u aerotunelu T-38

U radu je data analiza uticaja držača modela na rezultate merenja u subsoničnom i transoničnom radnom delu aerotunela T-38. Razmatrana su dva tipa držača modela, prav repni i *Z* držač. Dat je oblik držača i veličina uticaja za neke posebne slučajeve. Osim na koeficijentu aksijalne sile C_A, glavni uticaj je na koeficijentu momenta propinjanja C_m. U radu je dat opis procedure za eliminisanje ovog neželjenog efekta.

Ključne reči: aerodinamički tunel, aerodinamičko ispitivanje, aerodinamički model, aerodinamički koeficijenti, subsonično strujanje, transonično strujanje.

Влияние Z-стойки модели на результаты измерения в аэродинамической трубе Т-38

В настоящей работе приведён анализ влияния стойки модели на результаты измерения в дозвуковой и в околозвуковой рабочих частях аэродинамической трубы Т-38. Здесь рассмотрены два типа стоек модели, фасонные как прямой хвост и *Z* - стойка. Тоже приведена конфигурация стойки и степень влияния для некоторых особых случаев. Кроме влияния на коэффициенте осевой силы C_a главное влияние оказывается на коэффициенте момента тангажа C_m. В работе описана методика для устранения этого ненужного и нежелательного эффекта.

Ключевые слова: аэродинамическая труба, аэродинамическое исследование, аэродинамическая модель, аэродинамические коэффициенты, дозвуковой поток, околозвуковой поток.

Interférence du support du modèle sur les résultats des mesurements dans la soufflerie aérodynamique T-38

Dans ce papier on donne l'analyse de l'interférence du support de modèle sur les résultats des mesurements effectués dans la chambre d'expérience subsonique et transsonique de la soufflerie aérodynamique T-38. On a considéré deux types de supports du modèle: support normal arrière et celui en forme de *Z*. Pour certains cas particuliers on a donné la forme du support ainsi que la magnitude de l'interférence. Excepté l'interférence sur le coefficient de la force axiale C_a, l'interférence principale est sur le coefficient du moment de tangage C_m. On a présenté aussi la description de la procédure pour éliminer cet effet indésirable.

Mots clés: soufflerie aérodynamique, essai aérodynamique, modèle aérodynamique, coefficients aérodynamiques, courant supersonique, courant transsonique.